Time-varying modal parameters identification in the modal domain

M. Bertha [1], **J.-C. Golinval** [1]
[1] University of Liège, Aerospace & Mechanical Engineering Department,
Allée de la Dcouverte 9, B-4000, Liège 1, Belgium
e-mail: **mathieu.bertha@ulg.ac.be**

Abstract

In a previous paper, we applied multivariate Autoregressive Moving-Average (ARMA) models coupled with a basis functions approach to perform the modal identification of time-varying structures. Thanks to the multivariate modelling, it is possible to get modal parameters, including mode shapes, at any time instant. The drawback is that, in order to get the varying modal parameters, an eigenvalue decomposition of a varying companion matrix is required for each time step. To tackle this problem, an alternative parameterization is chosen to switch from the ARMA domain to the modal domain. There are several advantages to use such a parameterization. First, the number of parameters may be reduced in some cases, which is in line with the parsimony principle. Next, because the modal parameters appear explicitly in the modal domain parameterization, there is no need to perform an eigenvalue decomposition to obtain them.
The present paper proposes to perform that change in parameterization in the time-varying framework, always using the basis functions approach. The method is applied on an experimental laboratory structure.

1 Introduction

In the field of structural engineering, modal analysis plays a key role for design or monitoring purposes. Nowadays, we can say that the modal analysis of linear time invariant (LTI) dynamical systems is pretty mature, as well in time and frequency domain, with a large variety of identification methods. However, in practice, this LTI assumption can be easily violated. Indeed, structures may show non linear responses for some levels of excitation or simply be time-varying because of working conditions, parts of the structure in motion or even environmental conditions. In both cases, the structure loses its fixed set of linear modal parameters. In this present work, we will focus on the identification of linear time-varying dynamical systems.

Some methods already exist for the identification of such systems. The simpler idea is to study the system by analyzing it on successive short time windows, in which the system is assumed stationary and use classical methods adapted to time-invariant systems. One can cite for example [1] in which a short-time version of the stochastic subspace identification (SSI) method is used for the identification of a scaled model of a bridge with a moving load. In previous works [2, 3], we dealt with the nonstationary behavior of time varying structures using the Hilbert transform and the Hilbert Vibration Decomposition (HVD) method [4] that we expanded for the treatment of multivariate measurements. Another way to proceed is to create models in which the parameters are simply let free to variate with time or any other parameter. In such methods, the resulting identified parameters at time t corresponds to the ones of the structure in its fixed condition at time t. It can be shown that for slowly varying parameters, this method is a good approximation of the true varying parameters of the system [5, 6]. To manage this time variation, a elegant method to proceed is to expand the parameters of the system in a basis of known time functions. In that way, the parameters to identify are then the coefficients of the latter functions and the problem becomes time invariant. Such a method, among others, is presented in [7] for time-varying autoregressive (AR) models and applied in the field of the identification of dynamical systems with time-varying autoregressive moving-average (ARMA) models in [8, 9]. In [10], this kind of ARMA models are also used in the framework of multivariate measurements and we shown in [11] that using such a method, the mode shapes can be accurately estimated too.

In this paper, we propose to create a time-varying modal state-space model to track the varying modal parameters of an experimental structure. The paper is organized as follows. In Section 2, the model is presented as well as the way its identification is performed. Then, in Section 3 the experimental structure is presented and the results of the identification are shown.

2 Modal domain state-space parameterization

As previously mentioned, we use here a state-space parameterization in the modal domain. In that way, the parameter we estimate have a direct physical meaning (poles and mode shapes components). In case of time-varying systems, this approach has a direct advantage because it avoids the computation of the eigenvalues/vectors decomposition of the state transition matrix (or the related companion matrix in the case of a multivariate ARMA modeling) for any time sample.

To present the following identification method, let us start with an example in the linear time invariant case before showing the expansion of the model using the basis functions approach to deal with the invariant behavior. The state-space representation of a system is a very common representation in many fields such as control or model identification for example. In the present case we will deal with only external measurements on the structure, the input force is recorded by the acquisition system, but not used as input of the method to show that it can be used in output only conditions. In this case, the classical way to represent a system in a state-space form is composed of two equations, the *state equation* and the *output equation*.

$$\left\{ \begin{array}{rcl} \boldsymbol{x}[t+1] & = & \boldsymbol{F}\,\boldsymbol{x}[t] + \boldsymbol{K}\,\boldsymbol{e}[t] \\ \boldsymbol{y}[t] & = & \boldsymbol{C}\,\boldsymbol{x}[t] + \boldsymbol{e}[t] \end{array} \right. \tag{1}$$

in which

- $\boldsymbol{F}$ is the state-transition matrix,
- $\boldsymbol{x}$ is the state vector,
- $\boldsymbol{y}$ is the output vector (gathering the experimental measurements),
- $\boldsymbol{e}$ is the innovation vector, and
- $\boldsymbol{K}$ is the Kalman gain matrix.

Let us note that there are many ways to represent the same system in a state-space form. The way shown in (1) is called an *innovation form* because of the presence in the model of the *innovation vector*, $\boldsymbol{e}$, that contains all the information that cannot be predicted by the model using the past data [12]. There is also many ways to represent this innovation form using similarity transformations of the system.

The next step is to transform the state-space model (1) into a modal form. Performing an eigenvalues/eigenvectors decomposition of the state transition matrix $\boldsymbol{F}$

$$\boldsymbol{F} = \boldsymbol{V}\,\boldsymbol{A}\,\boldsymbol{V}^{-1} \tag{2}$$

the model (1) can be transformed into the following one

$$\left\{ \begin{array}{rcl} \boldsymbol{\eta}[t+1] & = & \boldsymbol{A}\,\boldsymbol{\eta}[t] + \boldsymbol{\Psi}\,\boldsymbol{e}[t] \\ \boldsymbol{y}[t] & = & \boldsymbol{\Phi}\,\boldsymbol{\eta}[t] + \boldsymbol{e}[t] \end{array} \right. \tag{3}$$

with

$$\begin{aligned}
\boldsymbol{\eta} &= \boldsymbol{V}^{-1}\boldsymbol{x}, && (4)\\
\boldsymbol{A} &= \boldsymbol{V}^{-1}\boldsymbol{F}\boldsymbol{V}, && (5)\\
\boldsymbol{\Phi} &= \boldsymbol{C}\boldsymbol{V}, && (6)\\
\boldsymbol{\Psi} &= \boldsymbol{V}^{-1}\boldsymbol{B}. && (7)
\end{aligned}$$

Note that with that model, we get some physical interpretation of the new parameters. Indeed, the $\boldsymbol{A}$ matrix is now a diagonal one gathering the discrete poles of the system and the $\boldsymbol{\Phi}$ matrix its mode shapes. Both appear in complex conjugated pairs. The $\boldsymbol{\eta}$ vector corresponds to the modal coordinates and the output equation of (3) is no more than the modal expansion of the response of the system. This kind of modal representation of the system was already used in [13] for example, making the link with its corresponding ARMA model.

In the following, we use a similar parameterization that we expand into a time-varying one but with a slight difference. The model (3) is made up with complex conjugated values for the poles and modes. To avoid treating such complex values, separating the real and imaginary parts of each parameter offers the possibility to work with only real values. This does not change anything to the modal decoupling of the model but slightly change the model matrices.

The matrix $\boldsymbol{A}$ is no more diagonal but is now a block-diagonal matrix

$$\boldsymbol{A} = \begin{bmatrix} \boldsymbol{A}_1 & & & \\ & \boldsymbol{A}_2 & & \\ & & \ddots & \\ & & & \boldsymbol{A}_n \end{bmatrix} \tag{8}$$

in which each block is formed as follows

$$\boldsymbol{A}_i = \begin{bmatrix} a_i & b_i \\ -b_i & a_i \end{bmatrix} \tag{9}$$

with a_i and b_i being the real and imaginary parts of the i^{th} pole, respectively. The left and right mode shapes in $\boldsymbol{\Phi}$ and $\boldsymbol{\Psi}$ are also built with real and imaginary parts of each mode. This is explained in detail in [14] for example.

2.1 Identification of the state-space model

To perform the identification of the model, a *prediction error* (PE) is minimized iteratively by nonlinear optimization. If we denote by a hat ($\hat{}$) the estimates of the model (the output estimate $\hat{\boldsymbol{y}}[t]$ and the state estimate $\hat{\boldsymbol{\eta}}[t]$) we have

$$\left\{ \begin{aligned} \hat{\boldsymbol{\eta}}[t+1,\boldsymbol{\theta}] &= \boldsymbol{A}\,\hat{\boldsymbol{\eta}}[t,\boldsymbol{\theta}] + \boldsymbol{\Psi}\,(\boldsymbol{y}[t] - \hat{\boldsymbol{y}}[t,\boldsymbol{\theta}]) \\ \hat{\boldsymbol{y}}[t,\boldsymbol{\theta}] &= \boldsymbol{\Phi}\,\hat{\boldsymbol{\eta}}[t,\boldsymbol{\theta}] \end{aligned} \right. , \tag{10}$$

or equivalently

$$\left\{ \begin{aligned} \hat{\boldsymbol{\eta}}[t+1,\boldsymbol{\theta}] &= (\boldsymbol{A} - \boldsymbol{\Psi}\boldsymbol{\Phi})\,\hat{\boldsymbol{\eta}}[t,\boldsymbol{\theta}] + \boldsymbol{\Psi}\,\boldsymbol{y}[t] \\ \hat{\boldsymbol{y}}[t,\boldsymbol{\theta}] &= \boldsymbol{\Phi}\,\hat{\boldsymbol{\eta}}[t,\boldsymbol{\theta}] \end{aligned} \right. . \tag{11}$$

The error to be minimized is the difference between the measured and predicted output:

$$\boldsymbol{e}[t,\boldsymbol{\theta}] = \boldsymbol{y}[t] - \hat{\boldsymbol{y}}[t,\boldsymbol{\theta}] \tag{12}$$

and it is minimized in a least squares sense, i.e. minimize the following cost function

$$\begin{aligned} V(\boldsymbol{\theta}) &= \frac{1}{N} \textstyle\sum_{t=1}^{N} \boldsymbol{e}[t,\boldsymbol{\theta}]^T \boldsymbol{e}[t,\boldsymbol{\theta}] \\ &= \frac{1}{N} \boldsymbol{E}(\boldsymbol{\theta})^T \boldsymbol{E}(\boldsymbol{\theta}). \end{aligned} \tag{13}$$

with $\boldsymbol{E}(\boldsymbol{\theta}) = \left[\boldsymbol{e}[1]^T\, \boldsymbol{e}[2]^T\, \cdots\, \boldsymbol{e}[N]^T\right]^T$ gathering all the residual terms in a single vector.

To proceed to the minimization of (13), a classical *Levenberg-Marquardt* optimization scheme is chosen in this work. In this iterative method, the set of parameters is updated from one iteration to another

$$\boldsymbol{\theta}^{(k+1)} = \boldsymbol{\theta}^{(k)} + \boldsymbol{d} \tag{14}$$

where $\boldsymbol{d}$ is the update to the vector of parameters. This update is obtained by taking the derivative of the cost function with respect to each of the parameters and it is solution of the following equation:

$$\left(\boldsymbol{J}^T \boldsymbol{J} + \lambda \boldsymbol{I}\right) \boldsymbol{d} = \boldsymbol{J}^T \boldsymbol{E} \tag{15}$$

in which $\boldsymbol{J}$ is the Jacobian of the residual vector and λ is the Marquardt parameter regularizing the equation. Note that the Levenberg-Marquardt algorithm is a balance between the Gauss-Newton method ($\lambda = 0$) and the gradient method ($\lambda \to \infty$). The calculation of the Jacobian matrix represents the major task of the algorithm. Taking the derivative of $\boldsymbol{E}(\boldsymbol{\theta})$ with respect to the $\boldsymbol{\theta}$ vector, we have

$$\boldsymbol{J} = \frac{\partial \boldsymbol{E}(\boldsymbol{\theta})}{\partial \boldsymbol{\theta}^T} = -\frac{\partial \hat{\boldsymbol{Y}}(\boldsymbol{\theta})}{\partial \boldsymbol{\theta}^T} \tag{16}$$

if $\hat{\boldsymbol{Y}}(\boldsymbol{\theta}) = \left[\hat{\boldsymbol{y}}[1]^T\, \hat{\boldsymbol{y}}[2]^T\, \cdots\, \hat{\boldsymbol{y}}[N]^T\right]^T$. That means that the Jacobian matrix is computed by calculating the derivative of the output estimate with respect to all the parameters. All that derivatives can be analytically computed as the realization of other state space models. In fact, introducing first a new variable $\hat{\boldsymbol{z}}[t] = \frac{\partial \hat{\boldsymbol{\eta}}[t,\boldsymbol{\theta}]}{\partial \theta_i}$ and considering (11), we have the following cases

- If θ_i belongs to the $\boldsymbol{A}$ matrix :

$$\left\{ \begin{aligned} \hat{\boldsymbol{z}}[t+1] &= (\boldsymbol{A} - \boldsymbol{\Psi}\boldsymbol{\Phi})\ \hat{\boldsymbol{z}}[t] + \boldsymbol{E}_{k,l}\, \hat{\boldsymbol{\eta}}[t,\boldsymbol{\theta}] \\ \frac{\partial \hat{\boldsymbol{y}}[t,\boldsymbol{\theta}]}{\partial \theta_i} &= \boldsymbol{\Phi}\, \hat{\boldsymbol{z}}[t] \end{aligned} \right. , \tag{17}$$

- If θ_i belongs to the $\boldsymbol{\Phi}$ matrix :

$$\left\{ \begin{aligned} \hat{\boldsymbol{z}}[t+1] &= (\boldsymbol{A} - \boldsymbol{\Psi}\boldsymbol{\Phi})\ \hat{\boldsymbol{z}}[t] - \boldsymbol{\Psi}\boldsymbol{E}_{k,l}\, \hat{\boldsymbol{\eta}}[t,\boldsymbol{\theta}] \\ \frac{\partial \hat{\boldsymbol{y}}[t,\boldsymbol{\theta}]}{\partial \theta_i} &= \boldsymbol{\Phi}\, \hat{\boldsymbol{z}}[t] + \boldsymbol{E}_{k,l}\, \hat{\boldsymbol{\eta}}[t,\boldsymbol{\theta}] \end{aligned} \right. , \tag{18}$$

- If θ_i belongs to the $\boldsymbol{\Psi}$ matrix :

$$\left\{ \begin{aligned} \hat{\boldsymbol{z}}[t+1] &= (\boldsymbol{A} - \boldsymbol{\Psi}\boldsymbol{\Phi})\ \hat{\boldsymbol{z}}[t] - \boldsymbol{E}_{k,l}\boldsymbol{\Phi}\, \hat{\boldsymbol{\eta}}[t,\boldsymbol{\theta}] + \boldsymbol{E}_{k,l}\, \boldsymbol{y}[t] \\ \frac{\partial \hat{\boldsymbol{y}}[t,\boldsymbol{\theta}]}{\partial \theta_i} &= \boldsymbol{\Phi}\, \hat{\boldsymbol{z}}[t] \end{aligned} \right. , \tag{19}$$

where $\boldsymbol{E}_{k,l}$ is a single entry matrix of appropriate dimension in which all components are null but one equal to one at the $(k,\, l)$ component corresponding to the position of the θ_i parameter in the matrix. It means that the Jacobian matrix is populated with a series of state-space realizations.

2.2 Time-varying expansion of the model

When the system under study loses its time invariant properties, its identification becomes harder. However, if the rate of change of the system properties is slow with respect to its dynamics, the modal parameters we get as considering for any time t its current configuration as fixed are a good approximation of the true time-varying parameters. This is what is called the *frozen time* approach (see [6]).

We have now to introduce this time variation into our model. To do it, we use here a *basis function expansion* of our parameters. The method is explained in [7] for time-varying AR models and used with ARMA models for the identification of mechanical systems in [9, 8] with a lot of detail. If we gather all the parameters of the model (in $\boldsymbol{A}[t]$, $\boldsymbol{\Phi}[t]$ and $\boldsymbol{\Psi}[t]$) into a parameter vector $\boldsymbol{\theta}[t]$, then each of these parameters are expanded in a previously chosen set of time functions $f[t]$, i.e.

$$\theta_i[t] = \sum_{j=1}^{n_f} \theta_{i,\,j}\, f_j[t]. \tag{20}$$

In that way, the parameters to be identified are now the $\theta_{i,\,j}$ coefficients which are time-invariant because the time variation is now kept by the chosen basis functions.

The identification of all the $\theta_{i,\,j}$ coefficients is performed exactly in the same way as explained in Section 2.1 but considering now the multiplication between the various signals and the basis functions.

3 Experimental identification of a laboratory test structure

3.1 Test setup

The experimental setup studied in this work is a mass-varying system shown in Figure 1. It is made up of a doubly supported beam on which a mass is moving, just like a bridge with a varying traffic load [8, 1]. The beam is a 2.1-meter long aluminum beam weighting approximately 9 kilograms. The moving mass is a 3.5-kilograms block of steel mounted on small wheels. The ratio between the masses of the two parts is high enough to observe a significant change in the dynamic properties of the system depending on the position of the mass. The whole system is supported by springs in order to put the excitation system and it is monitored by twelve accelerometers along the beam. The system is excited by a shaker with a random force in order to excite all the modes.

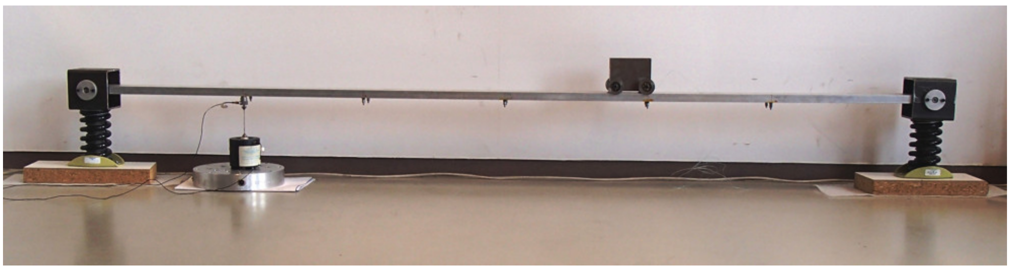

Figure 1: The supported beam on which the mass is moving.

3.2 First LTI identification

In order to have a reference set of results for further comparison, a first analysis is performed on the supported beam subsystem (the moving mass is not considered here). The analysis is performed in the Test.Lab [15] software using the PolyMax method [16]. The obtained result in term of stabilization diagram is illustrated in Figure 2. In addition Table 1 and Figure 3 show the results in terms of frequency, damping and mode shapes.

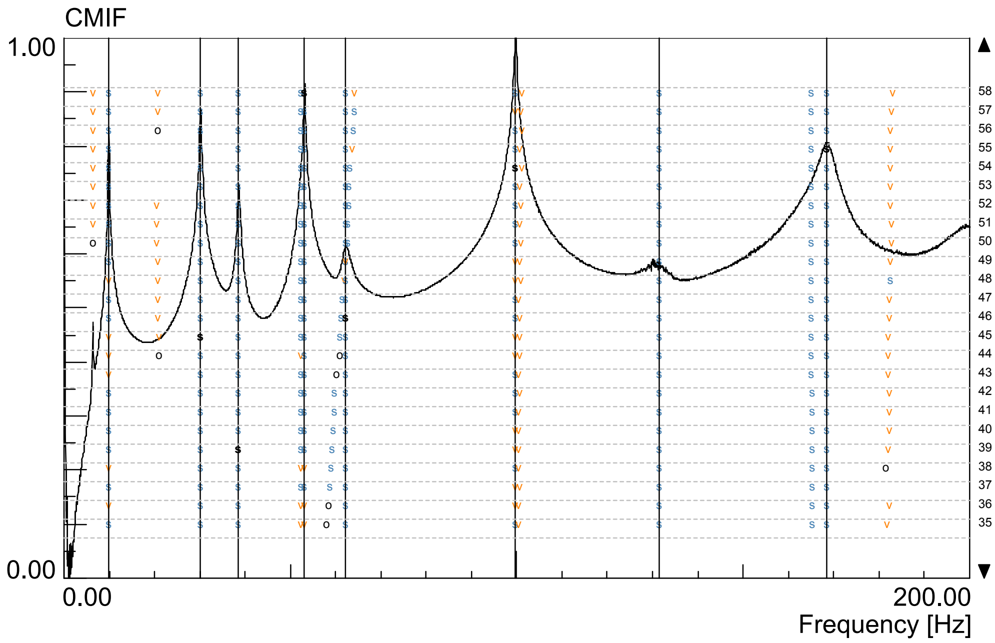

Figure 2: Stabilization diagram of the beam-only subsystem.

Mode #	f_r [Hz]	ζ_r [%]
1	9.86	0.32
2	30.12	0.52
3	38.6	0.65
4	53.14	0.28
5	62.17	1.57
6	99.70	0.28
7	131.57	2.039
8	168.60	0.99

Table 1: Frequencies and damping ratio's up to 200 Hz in the linear time invariant case.

3.3 LTV identification

Let us now continue with the identification of the system when the mass is travelling. Globally, the modification in the system is based on an addition of a mass which affects the inertia forces. If we make travel the mass on the beam during an experiment, we may have a first idea of what happens by looking to a time-frequency decomposition of an output measurement. Figure 4 shows such a response of the system using a wavelet decomposition. It can be seen that the frequencies of each mode generally decrease because of the presence of additional inertia forces brought by the mass. It can also be observed that at some time instants, the frequencies come back to their upper value. This corresponds for each mode when the mass passes at nodes of vibration. At that particular locations, because there is no deflection of the mode shape, the mass does not work on the mode and its frequency comes back to the one corresponding to the LTI subsystem. Of course that particular instants are different from modes to modes.

The present identification relies on an iterative optimization scheme, therefore, it has to be initialized at the first step. Because we performed an analysis of the system without the moving mass (Section 3.2) we can use these results as first guess for the optimization. They are put as coefficients of the first function which is a unitary function and all the other parameters are put at zero. If such initial results are not available, it is always possible to compute an initial set of parameters by performing an LTI analysis on a short portion of the response by a standard (output only) modal analysis method.

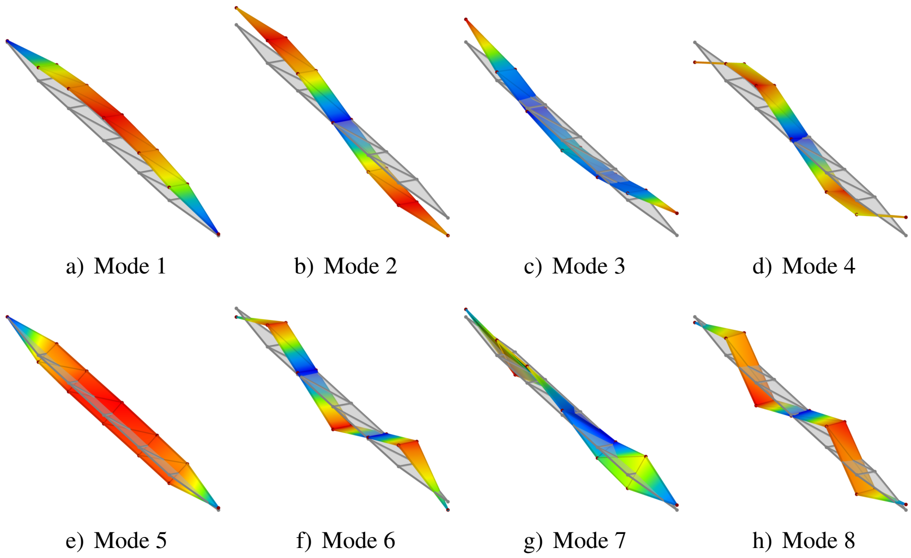

Figure 3: Complete set of mode shapes up to 200 Hz in the linear time invariant case.

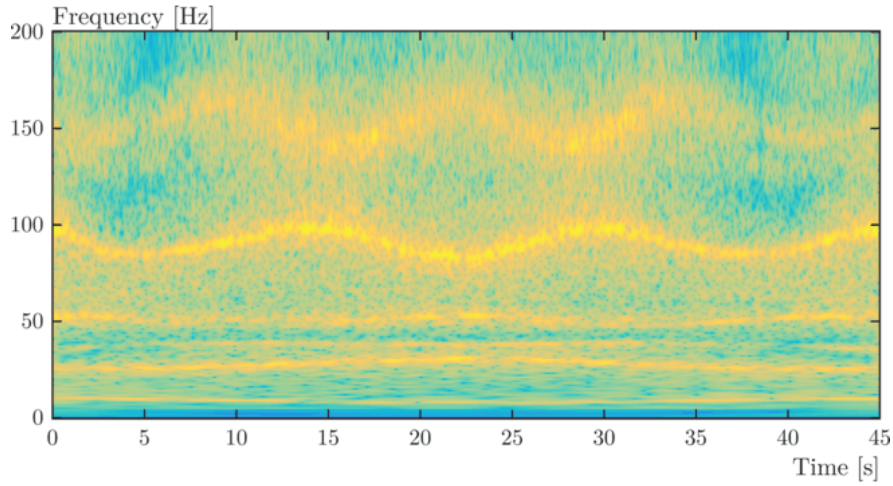

Figure 4: Wavelet transform of the output at the 3^{rd} sensor.

One point we have to deal with in the optimization problem is its complexity i.e. the number of parameters involved in the identification process. It is well known in non-convex optimization with the Levenberg-Marquardt (and the Newton familly algorithms) that the greater the number of parameters, the greater is the risk to converge to a local minimum. To tackle this problem, a graduated optimization strategy is chosen. It means that the initial (very-) complex problem is solved in a series of simpler optimization problems. An illustration of this way to solve the problem is shown in Figure 5. This method can be used in our case because of the chosen parameterization for the identification. Indeed, our parameterization being similar to the modal decomposition, it is possible to identify one or few modes at a time and retrieve their contribution to the response before continuing with the identification of one or few other modes. Of course, it is better to begin by the modes having the greater response because the optimization algorithms tries to minimize the residual response.

The first step of the identification begins with a reduced set of modes to identify, in order to reduce the complexity of the problem. Let us start with modes 1, 2, 3, 4 and 6. A series of identifications are launched. Here the model order (number of modes to identify) is fixed, but a parameter remains to be determined: the number of basis functions. 11 Chebyshev polynomials are used as basis functions, but this choice is not unique and other bases can be chosen such as Legendre polynomials, Fourier functions and so on. Figure

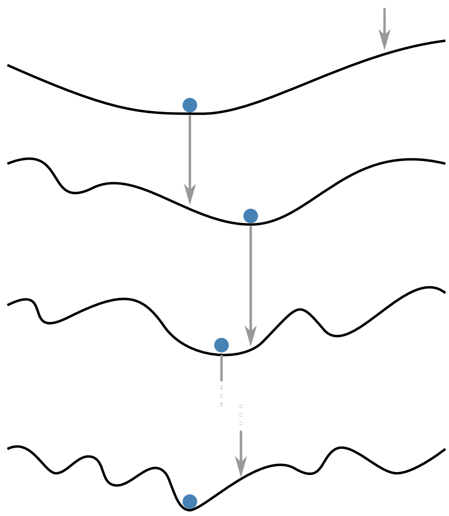

Figure 5: Illustration of the path to the solution by graduated optimization.

6a) shows the results of this first identification. Removing the contribution of the identified modes leads to the first residual response as shown in Figure 6b). It can be seen that the contribution of the previous modes is no more present.

The identification is then continued with the other modes, beginning by the last one which is the dominant one in the residual. To this aim, the number of polynomials has to be increased to 15. Once it is identified, it is removed from the signals just as before and the identification is finished by the identification of the two remaining modes which are the less excited of all the modes. The final set of results is shown in Figure 7 in terms of frequencies. However, the frequencies (more generally the whole pole) information is not the only result we can obtain. With the multivariate modeling the mode shapes can also be directly identified by the method. In Figure 8 the six bending modes of the structure are plotted for 4 time instants in the experimental data. The moving mass affects the mode shapes especially when it is located at an antinode. Conversely, as previously observed on the frequencies, when the mass is located at a node of vibration of a mode, its mode shape is not perturbed anymore and the mode shape comes back to a similar shape as the one it had in the LTI case. This is for example the case for modes 2, 4, and 8 at 22.5 seconds, when the mass is approximately around the center of the beam.

4 Conclusion

The paper presented a modal parameterization coupled with the basis functions approach for the identification of time-varying mechanical systems. It was shown how the optimization algorithm identifies the time-varying modal parameters of the laboratory test structure. The obtained results, the poles but also the mode shapes, are in good agreement with the physics behind the motion of the mass about the beam axis.

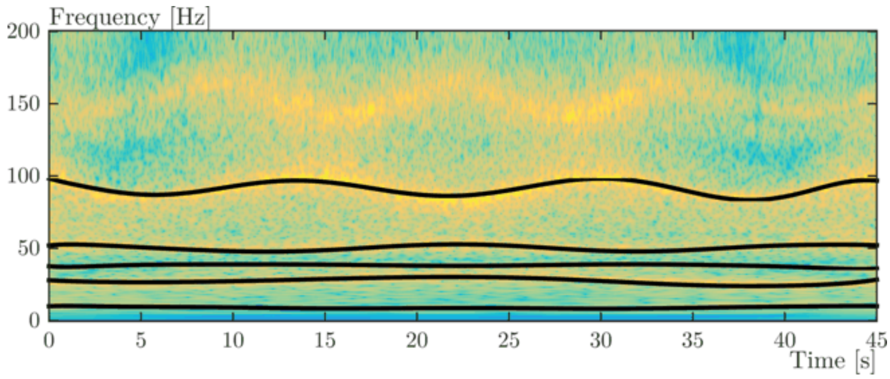

a) Identification of the 2nd, 3rd, 4th and 6th time-varying modes

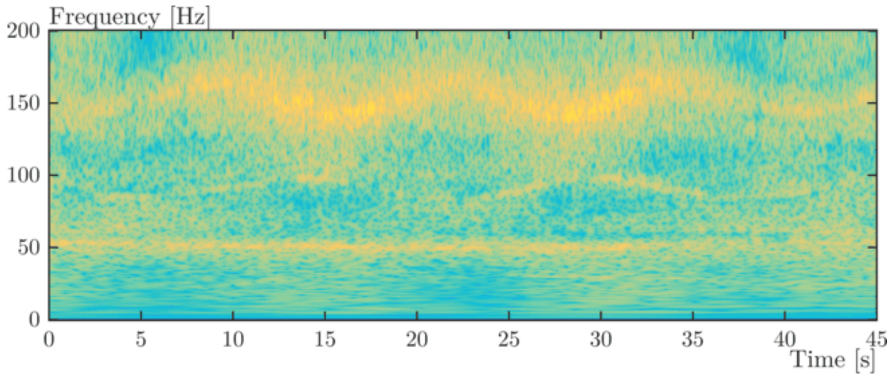

b) Residual after the first identification.

Figure 6: Time-varying identification of the structure.

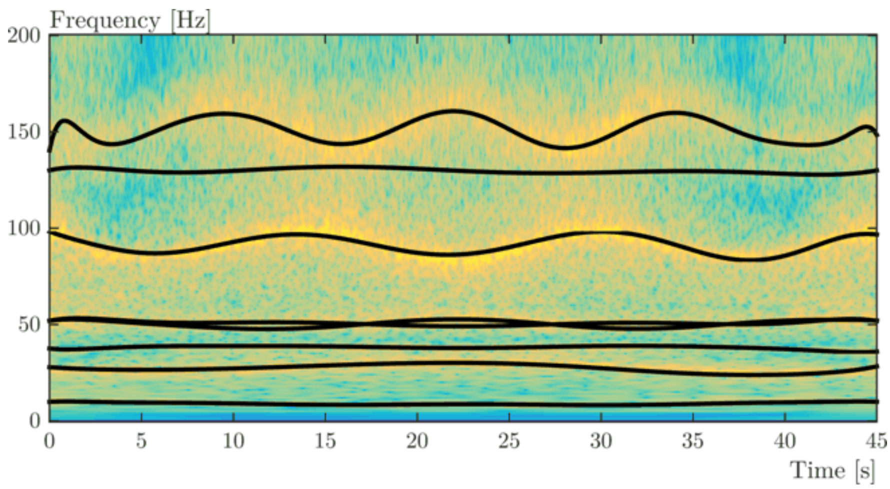

Figure 7: Complete set of identified modes.

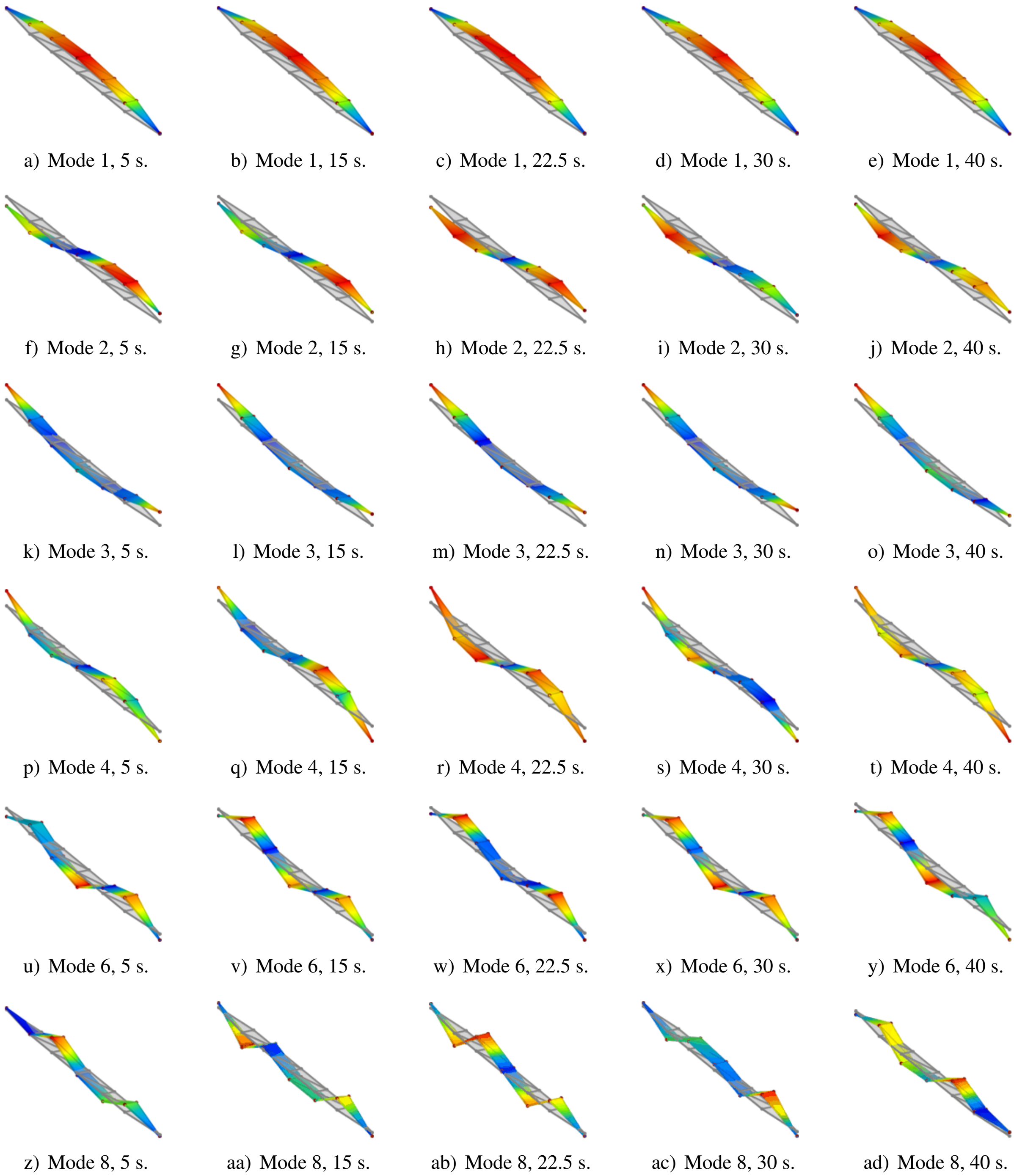

a) Mode 1, 5 s. b) Mode 1, 15 s. c) Mode 1, 22.5 s. d) Mode 1, 30 s. e) Mode 1, 40 s.

f) Mode 2, 5 s. g) Mode 2, 15 s. h) Mode 2, 22.5 s. i) Mode 2, 30 s. j) Mode 2, 40 s.

k) Mode 3, 5 s. l) Mode 3, 15 s. m) Mode 3, 22.5 s. n) Mode 3, 30 s. o) Mode 3, 40 s.

p) Mode 4, 5 s. q) Mode 4, 15 s. r) Mode 4, 22.5 s. s) Mode 4, 30 s. t) Mode 4, 40 s.

u) Mode 6, 5 s. v) Mode 6, 15 s. w) Mode 6, 22.5 s. x) Mode 6, 30 s. y) Mode 6, 40 s.

z) Mode 8, 5 s. aa) Mode 8, 15 s. ab) Mode 8, 22.5 s. ac) Mode 8, 30 s. ad) Mode 8, 40 s.

Figure 8: Time-varying mode shapes at four time instants.

References

[1] S. Marchesiello, S. Bedaoui, L. Garibaldi, P. Argoul, *Time-dependent identification of a bridge-like structure with crossing loads*, Mechanical Systems and Signal Processing, Vol. 23(6), 2009, pp. 2019–2028.

[2] M. Bertha, J.-C. Golinval, *Experimental modal analysis of a beam traveled by a moving mass using Hilbert Vibration Decomposition*, in *Proceedings of Eurodyn IX*, Porto, 2014.

[3] M. Bertha, J.-C. Golinval, *Identification of a Time-Varying Beam Using Hilbert Vibration Decomposition*, in *Proceedings of IMAC XXXII*, Orlando, 2014.

[4] M. Feldman, *Hilbert Transform Applications in Mechanical Vibration*, John Wiley & Sons, Ltd, Chichester, UK (2011).

[5] K. Zenger, R. Ylinen, *Poles and Zeros of Multivariable Lienar Time-Varying Systems*, in *Proceedings of the 15th IFAC World Congress* (2002).

[6] L.A. Zadeh, *Frequency analysis of variable networks*, in *Proceedings of IRE 27*, (1950), pp. 170–177.

[7] M. Niedzwiecki, *Identification of Time-Varying Processes*, John Wiley & Sons, Inc., New York (2000).

[8] A.G. Poulimenos, S.D. Fassois, *Parametric time-domain methods for non-stationary random vibration modelling and analysis — A critical survey and comparison*, Mechanical Systems and Signal Processing, Vol. 20(4), 2006, pp. 763–816.

[9] M.D. Spiridonakos, S.D. Fassois, *Non-stationary random vibration modelling and analysis via functional series time-dependent ARMA (FS-TARMA) models - A critical survey*, Mechanical Systems and Signal Processing, Vol. 47, 2014, pp. 175-224.

[10] M.D. Spiridonakos, S.D. Fassois, *Parametric identification of a time-varying structure based on vector vibration response measurements*, Mechanical Systems and Signal Processing, Vol. 23(6), 2009, pp. 2029–2048.

[11] M. Bertha, J.-C. Golinval, *Multivariate ARMA Based Modal Identification of a Time-varying Beam*, in *Proceedings of IMAC XXXIV*, Orlando, 2016.

[12] L. Ljung, *System Identification : Theory for the User*, 2nd ed., Prentice Hall, 1999.

[13] R. Brincker, P. Andersen, *ARMA models in modal space*, in *Proceedings of IMAC XVII*, 1999: pp. 330–334.

[14] M. Patil, *Decoupled second-order equations and modal analysis of a general nonconservative system*, in *Proceedings of the 41st Structures, Structural Dynamics, and Materials Conference and Exhibition*, Reston, Virigina (2000).

[15] LMS Test.Lab, http://www.plm.automation.siemens.com/en_us/products/lms/testing/test-lab/index.shtml.

[16] B. Peeters, H. Van Der Auweraer, P. Guillaume, J. Leuridan, *The PolyMAX frequency-domain method: a new standard for modal parameter estimation?*, Shock and Vibration, Vol 11, 2004, pp. 395–409.